sensors

MDPI

Article

0.5 V Multiple-Input Fully Differential Operational Transconductance Amplifier and Its Application to a Fifth-Order Chebyshev Low-Pass Filter for Bio-Signal Processing

Tomasz Kulej [1], Fabian Khateb [2,3,4] and Montree Kumngern [5,*]

[1] Department of Electrical Engineering, Czestochowa University of Technology, 42-201 Czestochowa, Poland; kulej@el.pcz.czest.pl
[2] Department of Microelectronics, Brno University of Technology, Technická 10, 601 90 Brno, Czech Republic; khateb@vutbr.cz
[3] Faculty of Biomedical Engineering, Czech Technical University in Prague, nám. Sítná 3105, 272 01 Kladno, Czech Republic
[4] Department of Electrical Engineering, Brno University of Defence, Kounicova 65, 662 10 Brno, Czech Republic
[5] Department of Telecommunications Engineering, School of Engineering, King Mongkut's Institute of Technology Ladkrabang, Bangkok 10520, Thailand
* Correspondence: montree.ku@kmitl.ac.th

Abstract: This paper presents a multiple-input fully differential operational transconductance amplifier (MI-FD OTA) with very low power consumption. To obtain a differential MOS pair with minimum supply voltage and minimum power consumption, the multiple-input bulk-driven MOS transistor operating in the subthreshold region is used. To show the advantage of the MI-FD OTA, a fifth-order Chebyshev filter was used to realize a low-pass filter capable of operating with a supply voltage of 0.5 V and consuming 60 nW at a nominal setup current of 3 nA. The proposed filter uses five MI-FD OTAs and five capacitors. The total harmonic distortion (THD) was 0.97% for a rail-to-rail sinusoidal input signal. The MI-FD OTA and the filter application were designed and simulated in the Cadence environment using a 0.18 µm CMOS process from TSMC. The robustness of the design was confirmed by Monte Carlo analysis and process, voltage, and temperature corner analysis.

Keywords: bulk-driven; multiple input MOS transistor; low-pass filter; low-voltage low-power CMOS

Citation: Kulej, T.; Khateb, F.; Kumngern, M. 0.5 V Multiple-Input Fully Differential Operational Transconductance Amplifier and Its Application to a Fifth-Order Chebyshev Low-Pass Filter for Bio-Signal Processing. *Sensors* **2024**, *24*, 2150. https://doi.org/10.3390/s24072150

Academic Editor: Cristoforo Marzocca

Received: 24 February 2024
Revised: 22 March 2024
Accepted: 25 March 2024
Published: 27 March 2024

1. Introduction

The operational transconductance amplifier (OTA) is a fundamental building block in analog signal processing. It has been used in a wide variety of applications, such as analog filters, audio amplifiers, data converters (D/A and A/D), modulators, instrumentation, etc. Extremely low-voltage supply and low-power integrated circuits are essential for battery-powered devices, portable and wearable biomedical electronics, IoT (Internet of Things) devices, and energy-autonomous integrated systems [1–9].

In the widely used bulk CMOS technology, several design techniques have been developed by designers to maintain acceptable circuit performance while the supply voltage (V_{DD}) moves toward the threshold voltage (V_{TH}) of the MOS transistor and even much lower, i.e., $V_{DD} \leq V_{TH}$ [1]. The most degraded parameter is the input voltage range, so techniques such as bulk-driven (BD), floating-gate (FG), quasi-floating gate (QFG), and multiple-input MOS transistors (MI-MOST) are good solutions to extend the input voltage range up to rail-to-rail at extremely low supply voltage [1–9].

OTA-C filters are widely used in signal processing applications and provide flexibility and electronic tunability compared to passive filters [10–20]. However, they have higher power consumption, and their structure is more complex. Therefore, special design considerations must be taken into account when using these filters for biosignal processing. Biosignals have the attributes of low amplitudes (µV–mV range) and low

frequencies ≤10 kHz. Thus, a high dynamic range (DR) and a high linearity are required to enhance the signal-to-noise ratio and to minimize the harmonic distortion of filters, respectively. A fully differential structure of the filter is required to obtain improved signal voltage swing and noise immunity.

Therefore, in this paper, a multiple-input fully differential OTA-C filter for biosignal processing is presented. The multiple-input MOS transistor is used to reduce the design complexity and to keep the number of active blocks as small as possible. The circuit operates in the subthreshold regime to enable reduced voltage supply and power consumption of the proposed OTA. In addition, to avoid increasing the chip area and power consumption, a simple bulk-driven common-mode feedback circuit (CMFB) is incorporated into the OTA current mirror structure. All this makes the circuit simple and capable of operating from a low-voltage supply with low power consumption and extended input voltage range.

The paper is organized as follows: Section 2 describes the circuit of the proposed MI-FD OTA, and the application of the proposed OTA in a fifth-order Chebyshev low-pass filter, Section 3 presents the simulation results, and Section 4 concludes the paper.

2. Circuit Description

2.1. Multiple-Input Fully-Differential OTA

The circuit symbol of the multiple-input fully differential OTA (MI-FD OTA) is shown in Figure 1. Compared to the standard circuit (Figure 1a), the MI-OTA possess N differential inputs; thus, its output current is a superposition of responses from each differential input, as expressed by (1). In other words, the output current is a sum of N currents, which are products of differential voltages at each differential input and the same transconductance g_m.

$$I_o = \sum_{i=1}^{N} g_m(V_{+i} - V_{-i}) \tag{1}$$

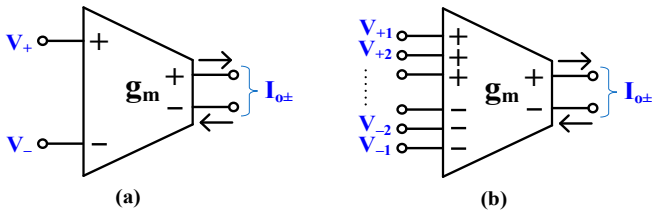

Figure 1. Electrical symbol of (**a**) fully differential OTA and (**b**) multiple-input fully differential.

The use of multiple-input OTAs increases the circuit versatility and reduces the number of active blocks used in some applications [8–10]. For instance, its application is especially advantageous in the design of OTA-C active filters.

The CMOS schematic of the multiple-input fully differential OTA proposed in this work is shown in Figure 2. In Figure 2a, a single-input (N = 1) core of the OTA is shown, while Figure 2b shows a complete version of the circuit with multiple inputs. Let us first consider the single-input core of Figure 2a. The proposed OTA exploits a classical current-mirror configuration, where the output currents of the differential stage (M_1, M_2, M_{11}, M_{12}) are transferred to the outputs O_+ and O_- via the set of unity-gain current mirrors (M_3–M_{10}, M_{13}, M_{14}).

The input stage exploits the concept of a non-tailed differential pair [21]. The gates of the input transistors M_1 and M_2 are biased by the diode-connected transistors M_{11}, M_{12}. All transistors have their bulk terminals connected to the input terminals V_+ and V_-. Note that in this configuration, $V_{GS1} = V_{GS11}$, $V_{BS1} = V_{BS11}$, $V_{GS2} = V_{GS12}$, and $V_{BS2} = V_{BS12}$. Assuming perfect symmetry and that $M_8 = M_B$ and $V_+ = V_-$, the drain currents of M_1 and M_2 are equal to $I_{D1,2} = (I_{set}/2)[(W/L)_{1,2}/(W/L)_{11,12}]$. This means that for common-mode signals ($V_+ = V_-$), while neglecting the second-order effects associated with the non-zero g_{ds} conductances of MOS devices, the currents $I_{D1} = I_{D2}$ remain constant, and the circuit is

insensitive to such signals. On the other hand, for differential signals, the circuit behaves as a classical long-tailed bulk-driven (BD) differential pair [15]. In the weak inversion region, assuming $I_{D1} = I_{set}/2$ at the operating point, its large-signal transfer characteristic can be expressed as follows [15]:

$$I_{D2} - I_{D1} = I_{set} \tanh\left(\frac{\eta(V_+ - V_-)}{2n_p U_T}\right) \quad (2)$$

where $\eta = g_{mb1,2}/g_{m1,2}$ is the bulk to gate transconductance ratio of the input transistors M_1 and M_2 at the operating point, n_p is the subthreshold slope factor for p-channel transistors and U_T is the thermal potential. As can be concluded from (2), the linear range of the input pair is extended by a factor of $1/\eta$, as compared to the classical GD differential pair.

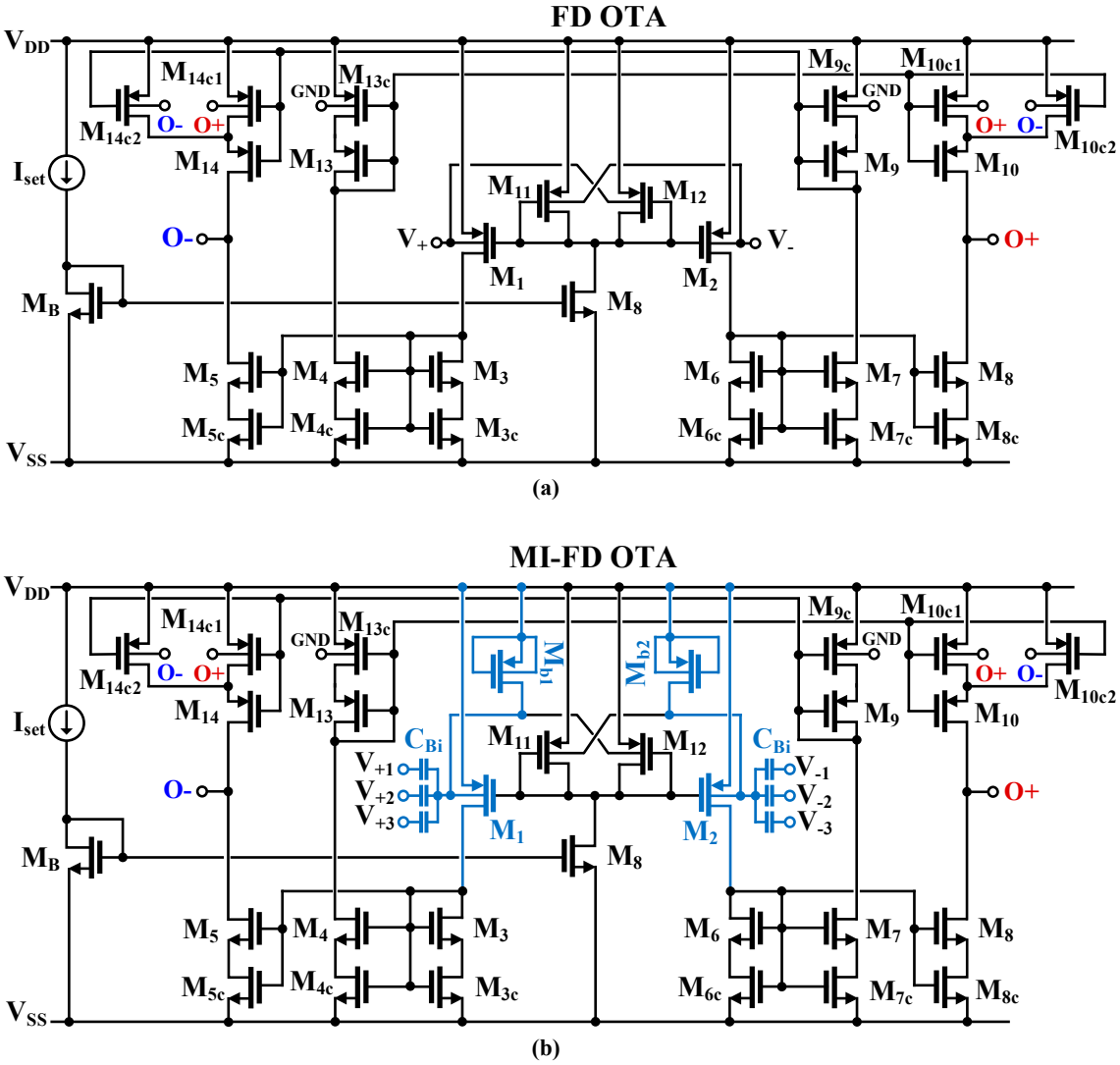

Figure 2. CMOS implementation of (**a**) fully differential OTA and (**b**) multiple-input fully differential OTA.

The small-signal transconductance of the input stage, g_{mi}, is equal to the bulk transconductance of the input transistors M_1 and M_2 and is given by:

$$g_{mi} = g_{mb1,2} = \eta \frac{I_{set}}{2n_p U_T} \quad (3)$$

Thus, the transistors M_{11} and M_{12} do not affect the input transconductance.

The unity-gain current mirrors of the OTA are based on self-cascode transistors M_i-M_{ic} (i = 3–10, 13, 14). The transistors M_{ic} operate in the triode region, with a relatively small voltage drop V_{ds}. Such a solution increases the output resistance of the OTA, and consequently its dc voltage gain, while not limiting its output voltage swing.

In order to stabilize the common-mode output level of this fully differential OTA, a simple BD common-mode feedback circuit (CMFB) is built into the structure of the p-channel current mirrors. Transistors M_{10c} and M_{14c} are split into two identical devices (c_1 and c_2), and their bulk terminals are connected to the outputs of the OTA. At the same time, the bulk terminals of M_{9c} and M_{13c} are connected to a reference voltage (GND in this case). When the output common-mode level of the OTA is increasing/decreasing with respect to GND, the drain currents of M_{10} and M_{14} are decreasing/increasing, thus compensating for the initial change of the common-mode level. Neglecting second-order effects, the CMFB does not affect the differential gain of the OTA. However, for large output amplitudes, such a simple CMFB introduces some distortion because variations of r_{dsc1} and r_{dsc2} are not symmetrical. Nevertheless, this effect is relatively weak for low V_{DD} (limited amplitude) and bulk-controlled transistors. Thanks to the proposed approach, we obtain a simple and sufficiently effective CMFB that does not consume additional power, does not increase the silicon area of the circuit, and, at the same time, does not limit the output voltage swing because it uses elements already existing in the circuit.

The output resistance of the OTA, determined for each single output, can be approximated by:

$$r_{out+/-} \cong (g_{m8/5} r_{ds8/5} r_{ds8c/rc}) || (g_{m10/14} r_{ds10/14} r_{ds10c/14c}) \quad (4)$$

where $r_{ds10/14c} = (r_{ds10/14c1}) || (r_{ds10/14c2})$. Thus, the output resistance of the OTA based on self-cascode transistors is increased by a factor of $g_{mi} r_{dsci}$, where i denotes the index of the MOS transistors associated with the output nodes O_+ and O_-.

The dc differential voltage gain of the OTA in Figure 2a can be expressed as:

$$A_{vo} = 2 g_{mi} r_{out+/-} \quad (5)$$

Thanks to the increased value of the output resistance $r_{out+/-}$, the value of A_{vo} is also increased, as opposed to the version with simple current mirrors.

The input-referred noise of the OTA is the same as for an OTA with the same topology, but with a BD differential pair, composed of transistors M_1, M_2 at the input, and biased with the same currents. Note that transistors M_{11} and M_{12} do not contribute to the output noise because their noise appears as a common-mode signal at the gates of M_1 and M_2.

Figure 2b shows the MI version of the proposed circuit. The multiple input is created by a capacitive divider composed of the capacitors C_{Bi}. Their values should be significantly larger than the parasitic capacitances of the MOS transistors but much lower than the external capacitances used, for example, to provide a required frequency characteristic of a filter. In this way, the MI-OTA can be realized without the use of additional differential amplifiers, thus simplifying the overall structure and saving power. Moreover, the input signal range is extended since the input signal is attenuated by the capacitive divider. The input terminals of the internal OTA, i.e., the bulk terminals of M_1 and M_2, must be properly biased for dc, which is conducted by the MOS transistors M_{b1} and M_{b2}. Since the transistors operate in a triode-cutoff region, with $V_{GS} = 0$, their r_{ds} resistances are very high; thus, together with the capacitances C_{Bi}, they create a high-pass (HP) filter with a very low cutoff frequency. Such a filter allows the dc component of a bio-signal to be removed as well. Further, at the operating point, $V_{DS11,12}$ is approximately equal to zero, which means $V_{BS1,2}$ and $V_{BS11,12}$ are equal to zero as well. This lowers the bulk currents of the input transistors $M_{1,2}$ and $M_{11,12}$.

The transmittance of the input HP filter from a single input can be expressed as:

$$\beta(s) = \beta_o \frac{\frac{s}{\omega_h}}{1 + \frac{s}{\omega_h}} \quad (6)$$

where ω_h is the cutoff frequency of the filter, given as:

$$\beta\omega_h = \frac{1}{R_{LARGE}C_\Sigma} \tag{7}$$

where R_{LARGE} is the r_{ds} resistance of M_{b1} and M_{b2}, $C_\Sigma = C_{B1} + C_{B2} + \ldots + C_{BN} + C_i$ is the sum of all capacitances C_{Bi} of the input capacitive divider, and C_i is the input capacitance of the internal OTA, seen from the bulk of M_1 (M_2).

The high-frequency gain β_o from the i-th input, with other inputs grounded, is given by:

$$\beta_o = \frac{C_{Bi}}{C_\Sigma} \tag{8}$$

For N = 3, and neglecting C_i, $\beta_o = 1/3$.

Taking into account the above considerations, the quasi-static transfer characteristic of the MI-OTA from the i-th input, with other inputs shorted to ground, and for frequencies higher than ω_h, can be expressed as:

$$I_{O+} = -I_{O-} = I_{set}\tanh\left(\beta_o\eta\frac{(V_{i+} - Vi_-)}{2n_pU_T}\right) \tag{9}$$

thus, the linear range of the OTA is enlarged $1/\beta_o$ times, as compared to the BD differential pair operating in a weak inversion, and $1/\beta_o\eta$ times as compared to a GD pair. Assuming N = 3, and 0.18 µm technology, $1/\beta_o = 3$ and $1/\beta_o\eta$ is typically around 10.

The small-signal transconductance of the MI-OTA from one differential input is consequently given by:

$$g_{mMI} = \beta_o\,\eta\frac{I_{set}}{2n_pU_T} \tag{10}$$

and is also lowered by the input capacitive divider, which also decreases the dc voltage gain.

The input capacitive divider also increases the input-referred noise of the MI OTA, which above the cutoff frequency ω_h can be expressed as:

$$\overline{v_{nMI}^2} = \frac{1}{\beta_o^2}\overline{v_n^2} \tag{11}$$

where $\overline{v_{nMI}^2}$ is the input noise of the MI-OTA determined from one differential input and $\overline{v_n^2}$ is the input-referred noise of the single-input OTA of Figure 2a, which is equal to the input noise of the OTA with the same topology and biasing currents, but with the input stage based on a classical BD differential pair. Note that the transistors M_{b1} and M_{b2} (R_{LARGE}) do not contribute to the total input noise since above ω_h, their noise is suppressed by the capacitances C_{Bi}.

As can be concluded from (11) and (9), due to the input capacitive divider, the input noise increases in the same proportion as the input linear range. This means that the dynamic range (DR) is the same with and without the input divider.

Concluding the above considerations, it is clear that the proposed MI-OTA shows increased versatility associated with the increased number of inputs. In addition, the input capacitive divider increases linear range, decreases the transconductance and dc voltage gain of the OTA, while its DR remains unchanged. At the same time, it performs the role of a HP filter, required in many biomedical applications to remove the dc component of the input signal.

2.2. Fifth-Order Chebyshev Low-Pass Filter

Figure 3 shows the fifth-order doubly terminated RLC ladder filter. The fifth-order Chebyshev low-pass prototype filter with 0.5 dB ripple was designed. Thus, the element values for the doubly terminated Chebyshev low-pass filter can be given as $R_S = R_L = 1\ \Omega$, $L_1 = L_2 = 1.2296$ H, $C_1 = C_5 = 1.7058$ F, and $C_3 = 2.5408$ F. To design the 250 Hz cut-off

frequency, the prototype element values of Figure 3 could be chosen as $L_1 = L_2 = 54.74$ kH, $C_1 = C_5 = 15.529$ pF, $C_3 = 23.131$ pF, while letting $R_S = R_L = 69.93$ MΩ.

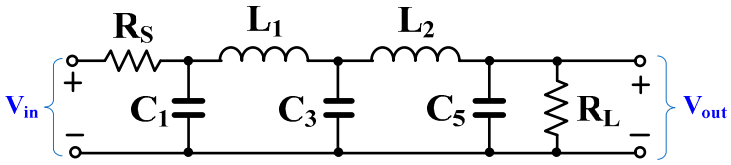

Figure 3. Fifth-order doubly terminated RLC ladder filter.

The proposed fifth-order Chebyshev low-pass filter using multiple-input OTAs is shown in Figure 4. By using multiple-input OTAs, five OTAs, and five capacitors are used. The resistors R_S and R_L can be implemented using the OTA, and their resistance values are given by $R_S = 1/g_{m1}$ and $R_L = 1/g_{m5}$, respectively. The floating inductors L_1 and L_2 are realized using gyrators and capacitors. Inductance values can be determined respectively by $L_1 = C_2/g_{m2}^2$ and $L_2 = C_4/g_{m4}^2$. The $g_{m1} - C_1$, $g_{m3} - C_3$, and $g_{m5} - C_5$ work as integrators. It should be noted that the structure of the filter is fully differential, which offers a high voltage swing compared with a single-ended filter, and the OTA-based circuit offers electronic tuning capability.

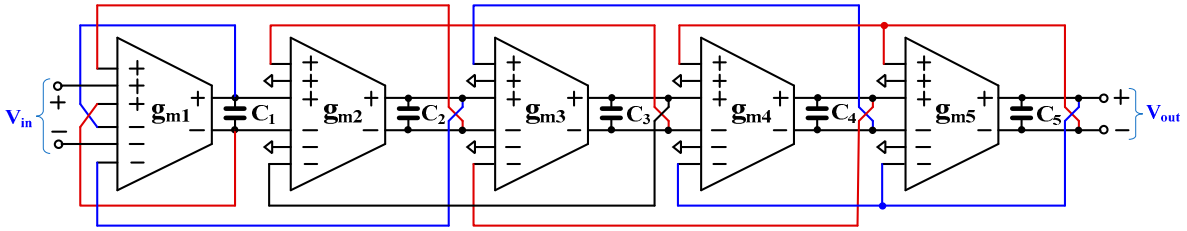

Figure 4. Proposed fifth-order Chebyshev low-pass filter.

The proposed fifth-order Chebyshev low-pass filter in Figure 4 is designed to obtain the cut-off frequency of 250 Hz; thus, the active and passive values are given by $g_{m1-5} = 7.54$ nS, $C_1 = C_5 = 7.764$ pF, $C_2 = C_4 = 5.597$ pF, and $C_3 = 11.565$ pF.

3. Simulation Results

The MI-FD OTA and the filter application were designed and simulated in the Cadence environment using a 0.18 µm CMOS process from TSMC. A supply voltage of 0.5 V ($V_{DD} = -V_{SS} = 0.25$ V) was employed in the simulation, and the nominal static power consumption of the transconductor with $I_{set} = 3$ nA was 12 nW. The transistor aspect ratio is shown in Table 1.

Table 1. Component parameters of the BD-OTA and MI-BD-OTA.

Transistor	W/L (µm/µm)
M_1, M_2	2 × 20/3
M_{11}, M_{12}	20/3
M_b, M_8	5/1
M_3–M_8, M_9–M_{12}	20/1
M_{3c}–M_{8c}	20/2
M_{9c}, M_{11c}	2 × 10/3
M_{10c1}, M_{10c2}, M_{11c1}, M_{11c2}	10/3
M_{b1}, M_{b2}	5/6
$C_B = 0.5$ pF	

The output current versus input voltage over the tuning range is shown in Figure 5. To obtain the dynamic characteristics of the BD-OTA and MIBD-OTA, a sine wave of amplitude 0.5 V at 200 Hz was applied to their inputs. Figure 5 shows the improved linearity of the MIBD-OTA compared with the BD-OTA with various setting currents I_{set} = (3, 6, 12, 24) nA.

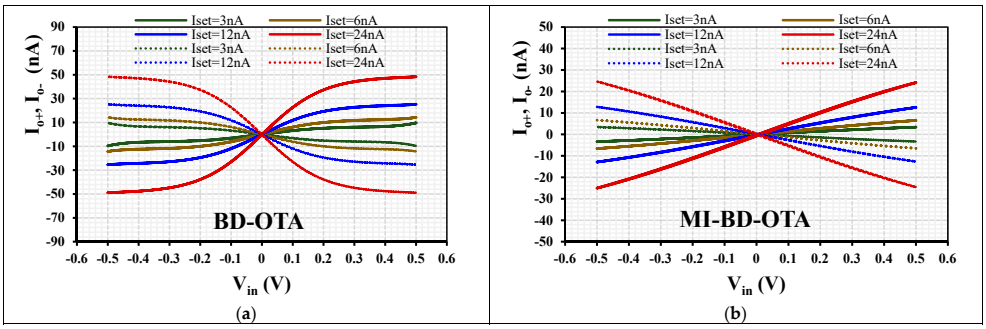

Figure 5. The output current I_{o+} and I_{o-} (dashed line) versus input voltage V_{in} over the tuning range of the (**a**) BD-OTA and (**b**) MIBD-OTA with different setting currents.

Figure 6 shows the transconductance AC characteristics of the BD-OTA and MI-BD-OTA with different tuning currents I_{set} = (3, 6, 12, 24) nA. The transconductances were (−149, −144, −137.8, −132.2) dB and (−162.4, −156.7, −150.9, −139.6) dB, respectively. As can be seen, due to the high-pass filter created at the input of the MI-BD-OTA, the low cutoff frequency is around 1.5 Hz. This can be further reduced if needed by increasing the M_b resistance.

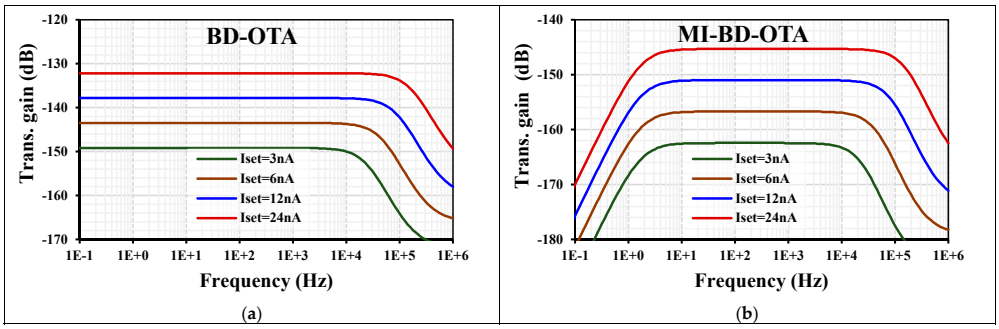

Figure 6. The transconductance AC characteristic of the (**a**) BD-OTA and (**b**) MIBD-OTA with different setting currents.

The equivalent input noise ($\mu V/\sqrt{Hz}$) of the (a) BD-OTA and (b) MI-BD-OTA is shown in Figure 7. The noise value was 2.51 µV and 11.5 µV at 100 Hz for the BD-OTA and MI-BD-OTA, respectively.

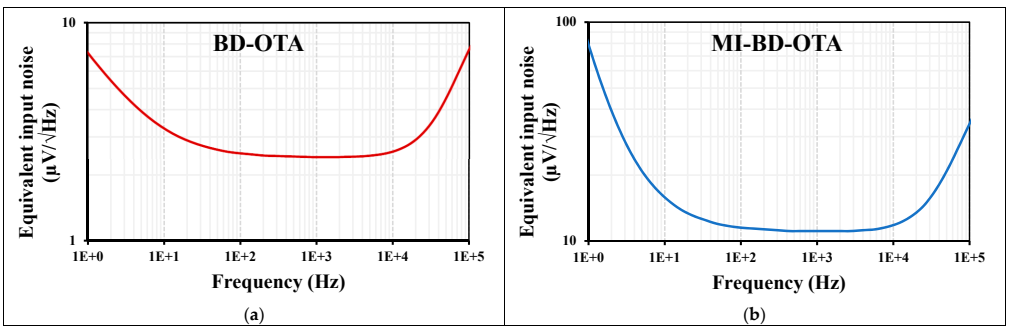

Figure 7. The equivalent input noise ($\mu V/\sqrt{Hz}$) of the (**a**) BD-OTA and (**b**) MIBD-OTA.

The AC transconductance characteristic from Figure 6b with I_{set} = 3 nA was replicated using 200 Monte-Carlo (MC) runs and process, voltage, and temperature (PVT) corners. The

transconductance value at 100 Hz varied from −163.6 to −161.2 dB using MC. The MOS transistor process corners were fast-fast, fast-slow, slow-fast, and slow-slow. The MIM capacitor corners were fast-fast and slow-slow, and the transconductance varied from −162.9 to −161.9 dB. The low cutoff frequency varied from 0.5 to 6.7 Hz. For the voltage supply corners $V_{DD} \pm 10\%V_{DD}$, the transconductance was −162.4 dB. The temperature corners were −10 °C and 60 °C, and the transconductance varied from −163 to −161.5 dB, while the low cutoff frequency varied from 0.16 to 11 Hz. These results are shown respectively in Figure 8a–d. All these variations are acceptable and expected, given the subthreshold operation. In addition, thanks to the circuit's tunability, the desired transconductance value can be readjusted.

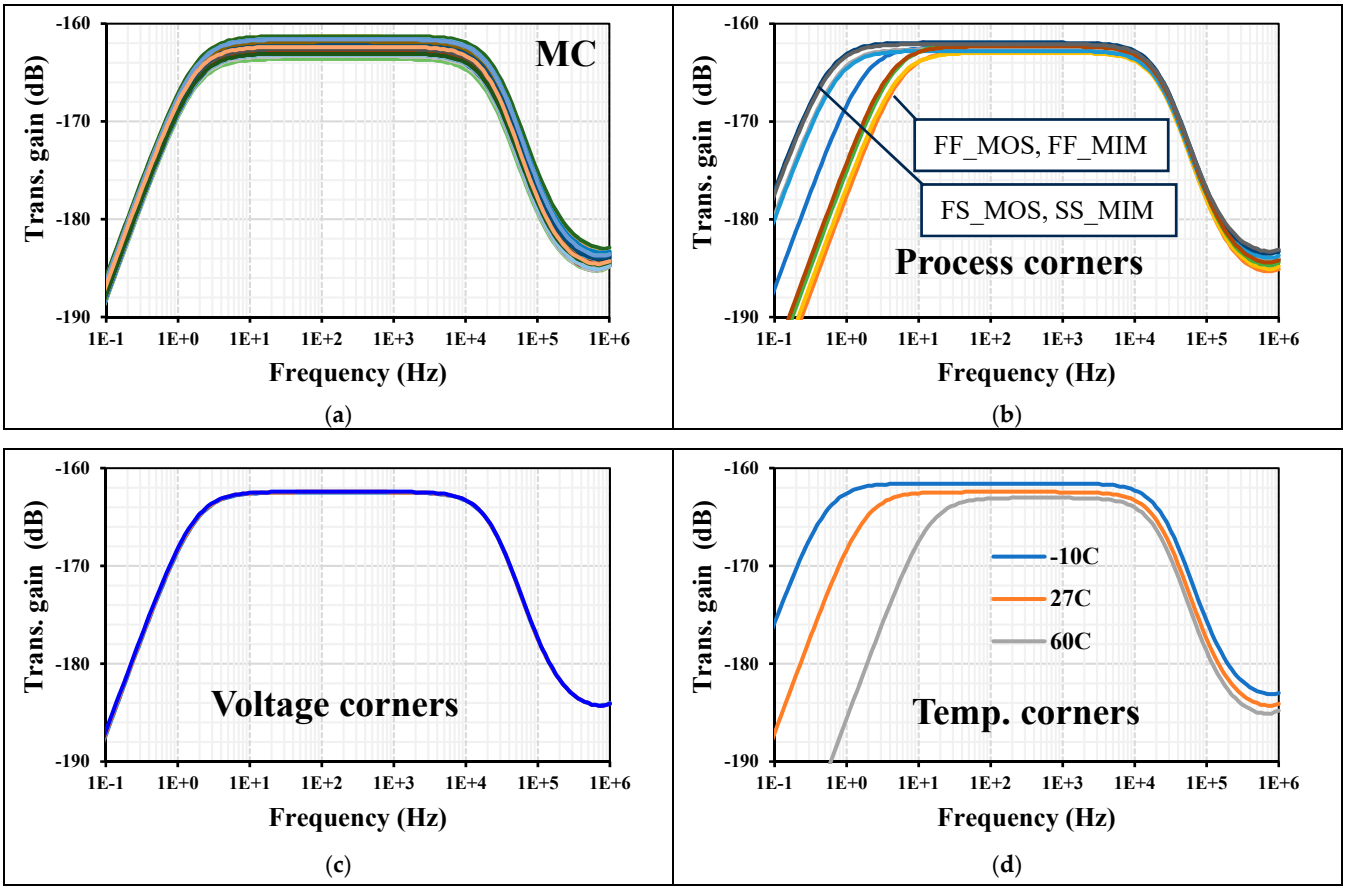

Figure 8. The transconductance AC characteristic of the MI-BD-OTA: (**a**) MC, (**b**) process, (**c**) voltage, and (**d**) temp. corners.

The power consumption of the filter for I_{set} = 3 nA was 5 × 12 nW = 60 nW. Figure 9a shows the frequency response of the LPF based on the RLC and the MI-BD-OTA with I_{set} = 3 nA. As can be seen, the two LP characteristics are close to each other, except for the low cut-off frequency at the sub-hertz level (50 mHz) created by the MI-BD-OTA input. This is an advantage in applications such as biosignals that require the removal of the DC component of the signal. The high cutoff frequencies are 242 Hz and 259 Hz, and the gain in the passband is −6 dB and −7.2 dB for the RLC and the filter based on MI-BD-OTA, respectively. Figure 9b shows the tuning capability of the filter with different I_{set} = (3, 6, 12, 24) nA. The high cutoff frequency was (259, 5094, 985, 1880) Hz, while the low cutoff frequency was around 50 mHz.

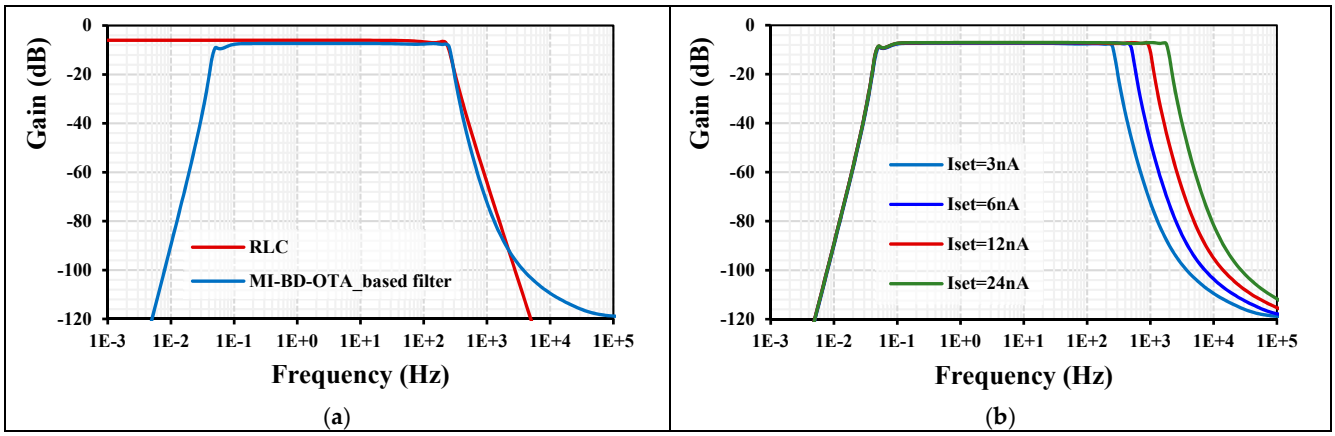

Figure 9. (**a**) The frequency response of the LPF and (**b**) the tuning capability of the LPF.

Figure 10a shows the transient response of the LPF, where the input signal was a sinewave with a rail-to-rail amplitude at 50 Hz. The spectrum of the output voltage is shown in Figure 10b and shows 0.97% total harmonic distortion (THD). Hence, the input signal can be rail-to-rail with less than 1% THD.

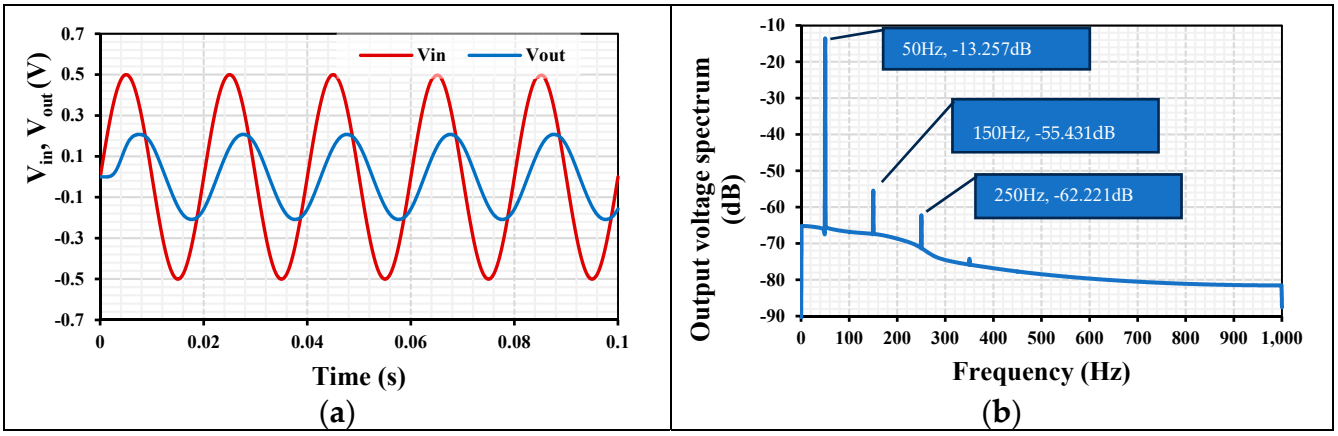

Figure 10. (**a**) The transient response of the LPF and (**b**) the output spectrum.

Figure 11 shows the total harmonic distortion of the output signal for different amplitudes of the input sine signals at 50 Hz. With an input amplitude of 400 mV and less, the THD was around 0.4%. The circuit can even operate beyond the rail-to-rail level with 3% THD for 600 mV amplitude.

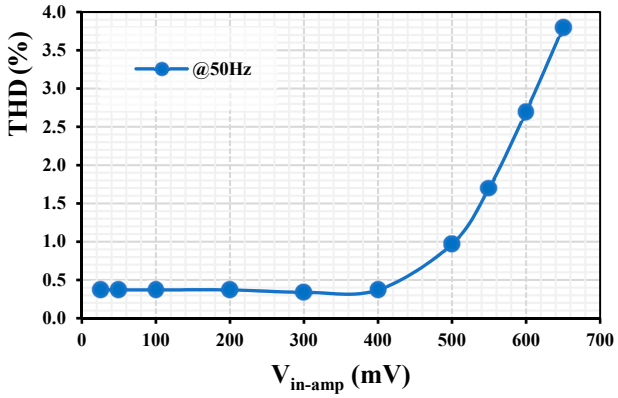

Figure 11. The THD of the LPF with different input amplitudes.

Figure 12 shows the equivalent output noise of the LPF. The integrated output noise in the range of 50 mHz to 259 Hz band was calculated to be 772 μV, giving a dynamic range of 53.2 dB.

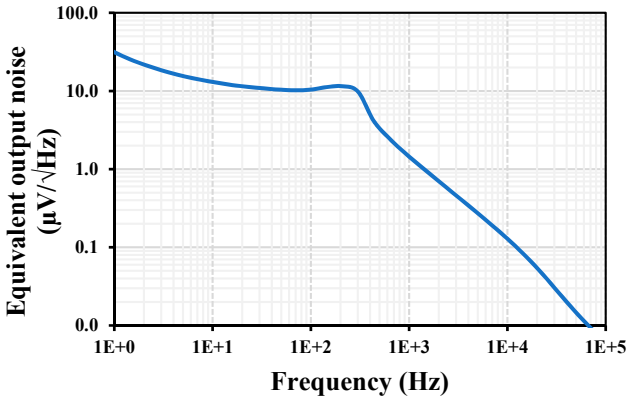

Figure 12. The equivalent output noise of the LPF.

To demonstrate the filtering function of the LPF with an ECG signal, Figure 13a shows the noisy input signal obtained by a clean ECG signal combined with 3 mV signals at 10 mHz and 500 Hz. Figure 13b shows the output signal of the filter where the low and high frequency signals have been filtered out.

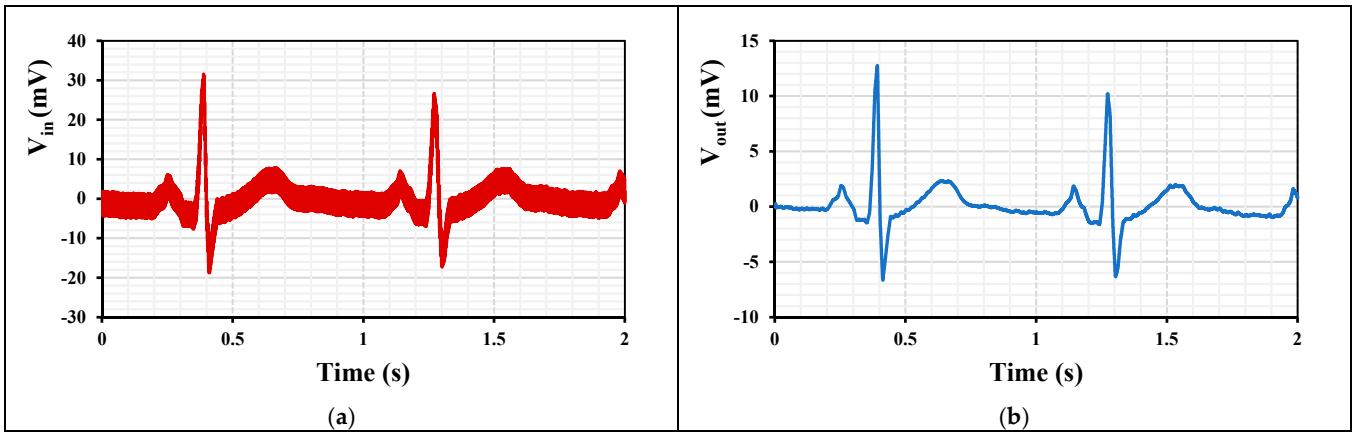

Figure 13. The transient response of the LPF to an ECG signal: (**a**) noisy input signal and (**b**) filtered output signal.

The proposed low-pass filter was compared with some previous works, as shown in Table 2. The fifth-order filters in [8,9,19,20,22,23] have been selected for comparison. It is clear that the MI-OTA-based filter offers a minimum number of active OTAs with a fully differential structure compared with [19,20,22,23]. Compared with [19,22,23], the proposed filter has low power consumption compared with [19,20,23], the proposed filter obtains low voltage capability, and compared with [8,19,20,22,23], the proposed filter provides LPF/BPF. Finally, compared with the BPF in [9], the proposed filter provides fully differential voltages, higher order (5 versus 3), with fewer active and passive components (5 versus 6). This is due to the internal high-pass filter created at the input of the MI-BD-OTA.

Table 2. Performance comparison of the proposed filter and previous fifth-order low-pass filters.

Symbol	This Work	Sensors (2020) [8]	IEEE ACCESS (2022) [9]	IEEE TCAS-II (2018) [19]	IEEE TBioCAS (2019) [20]	MEJ (2019) [22]	IEEE ACCESS (2023) [23]
V_{DD} [V]	0.5	0.5	0.5	1.0	1.0	0.25	1.0
Tech [µm]	0.18	0.18	0.18	0.18	0.18	0.13	0.065
V_{TH} [V]	0.5	0.5	0.5	0.5	0.5	0.44	0.3
Order (N)	5	5	3	5	5	5	5
Filter type	Chebyshev	Butterworth	Chebyshev	Butterworth	Butterworth	Butterworth	Butterworth
Filtering function	LPF/BPF	LPF	BPF	LPF	LPF	LPF	LPF
No. of active device	5 MI-OTAs	5-MI-OTAs	6-MI-OTAs	6 OTAs	6 OTAs	6 FDDTAs	11 OTAs
Architecture	G_m-C fully diff.	G_m-C fully diff.	G_m-C single-end	G_m-C fully diff.	G_m-C fully diff.	G_m-C fully diff.	G_m-C fully diff.
MOST technique	MIBD	MIGD	MIBD	GD	GD	GD	GD
BW/central freq. [Hz]	250	250	250	250	250	100	1×10^6
DR [dB]	53.2	63.24	60.4	49.9	61.2	57	50.54
Power (P) [nW]	60	34.65	60	350	41	603	167×10^3
FOM = P/(N × BW × DR) [pJ]	0.9	0.43	1.32	0.896	0.0286	1.7	0.66
LV operation capability = $V_{TH}/V_{DD} \times 100$ [%]	100	100	100	50	50	176	30
Area [mm^2]	NA	NA	0.036 (off chip cap.)	0.12	0.14	0.67 (off-chip cap.)	0.0164
Obtained results	Simulated	Simulated	Post-layout	Measured	Measured	Measured	Measured

Note: MIBD = Multiple-Input Bulk-Driven, GD = Gate-Driven, MIGD = Multiple-Input Gate-Driven, LPF = Low-Pass Filter, BPF = Band-Pass Filter.

4. Conclusions

This paper presents a 0.5 V multiple-input fully differential OTA and its application to a fifth-order Chebyshev low-pass filter for bio-signal processing. The circuit uses several design techniques and operates in the subthreshold region with a 0.5 V supply. It consumes power in the range of a few nanowatts while offering an extended input voltage range. The fifth-order Chebyshev low-pass filter, which uses the proposed multiple-input fully differential OTA as an active block, offers a minimum number of active devices and low design complexity. The circuit performance and applications have been confirmed by intensive simulation in the Cadence program.

Author Contributions: Conceptualization, T.K., F.K. and M.K.; methodology, T.K., F.K. and M.K.; software, T.K., F.K. and M.K.; validation, T.K., F.K. and M.K.; formal analysis, T.K., F.K. and M.K.; investigation, T.K., F.K. and M.K.; resources, T.K.; data curation, T.K., F.K. and M.K.; writing—original draft preparation, T.K., F.K. and M.K.; writing—review and editing, T.K., F.K. and M.K.; visualization, T.K., F.K. and M.K; supervision, T.K., F.K. and M.K.; project administration, T.K., F.K. and M.K.; funding acquisition, M.K. All authors have read and agreed to the published version of the manuscript.

Funding: This work was supported in part by the School of Engineering, King Mongkut's Institute of Technology Ladkrabang, under Grant 2566-02-01-030, and by the University of Defence within the Organization Development Project VAROPS.

Institutional Review Board Statement: Not applicable.

Informed Consent Statement: Not applicable.

Data Availability Statement: Data are contained within the article.

Conflicts of Interest: The authors declare no conflicts of interest.

References

1. Ballo, A.; Grasso, A.D.; Pennisi, S. Active load with cross coupled bulk for high-gain high-CMRR nanometer CMOS differential stages. *Int. J. Circuit Theory Appl.* **2019**, *47*, 1700–1704. [CrossRef]
2. Ballo, A.; Grasso, A.D.; Pennisi, S.; Susinni, G. A 0.3-V 8.5-µ a bulk-driven OTA. *IEEE Trans. Very Large Scale Integr. (VLSI) Syst.* **2023**, *31*, 1444–1448. [CrossRef]
3. Ballo, A.; Grasso, A.D.; Pennisi, S. 0.4-V, 81.3-nA bulk-driven single-stage CMOS OTA with enhanced transconductance. *Electronics* **2022**, *11*, 2704. [CrossRef]
4. Woo, K.-C.; Yang, B.-D. A 0.25-V rail-to-rail three-stage OTA with an enhanced DC gain. *IEEE Trans. Circuits Syst. II Express Briefs* **2020**, *67*, 1179–1183. [CrossRef]
5. Centurelli, F.; Sala, R.D.; Monsurró, P.; Tommasino, P.; Trifiletti, A. An ultra-low-voltage class-AB OTA exploiting local CMFB and body-to-gate interface. *AEU-Int. J. Electron. Commun.* **2022**, *145*, 154081. [CrossRef]
6. Ballo, A.; Grasso, A.D.; Pennisi, S. A 0.6 V bulk-driven class-ab two-stage OTA with non-tailed differential pair. *J. Low Power Electron. Appl.* **2023**, *13*, 24. [CrossRef]
7. Gangineni, M.; Ramirez-Angulo, J.; Paul, A.; Molinar-Solis, J.E.; Diaz-Sanchez, A.; Huerta-Chua, J.; Lavrova, O. ±0.15 V three-stage bulk-driven AB OTA with 36 MHzpF/µW and 55(V/µs)pF/µW small and large-signal figures of merit. *Electron. Lett.* **2023**, *49*, e13005. [CrossRef]
8. Kumngern, M.; Aupithak, N.; Khateb, F.; Kulej, T. 0.5 V fifth-order Butterworth low-pass filter using multiple-input OTA for ECG applications. *Sensors* **2020**, *20*, 7343. [CrossRef]
9. Khateb, F.; Prommee, P.; Kulej, T. MIOTA-based filters for noise and motion artifact reductions in biosignal acquisition. *IEEE Access.* **2022**, *10*, 14325–14338. [CrossRef]
10. Reed, R.D.; Geiger, R.L. A multiple-input OTA circuit for neural networks. *IEEE Trans. Circuits Syst.* **1989**, *36*, 767–770. [CrossRef]
11. Wyszynski, A.; Schaumann, R. Using multiple-input transconductors to reduce number of components in OTA-C filter design. *Electron. Lett.* **1992**, *28*, 217–220. [CrossRef]
12. Ramirez-Angulo, J.; Urquidi, C.A.; Gonzalez-Carvajal, R.; Torralba, A.; Lopez-Martin, A. A new family of very low-voltage analog circuits based on quasi-floating-gate transistors. *IEEE Trans. Circuits Syst. II Analog Digit. Signal Process.* **2003**, *50*, 214–220. [CrossRef]
13. Lopez-Martin, A.J.; Algueta, J.M.; Garcia-Alberdi, C.; Acosta, L.; Carvajal, R.G.; Ramirez-Angulo, J. Design of micropower class AB transconductors: A systematic approach. *Microelectron. J.* **2013**, *44*, 920–929. [CrossRef]
14. Martincorena-Arraiza, M.; De La Cruz-Blas, C.A.; Lopez-Martin, A.; Carlosena, A. Micropower class AB low-pass analog filter based on the super-source follower. *IEEE Trans. Circuits Syst. II Express Briefs* **2022**, *69*, 3684–3688. [CrossRef]
15. Kulej, T.; Khateb, F. Bulk-driven adaptively biased OTA in 0.18 um CMOS. *Electron. Lett.* **2015**, *51*, 458–460. [CrossRef]
16. Chatterjee, S.; Tsividis, Y.; Kinget, P. 0.5-V analog circuit techniques and their application in OTA and filter design. *IEEE J. Solid-State Circuits* **2005**, *40*, 2373–2387. [CrossRef]
17. Akita, I.; Wada, K.; Tadokoro, Y. A 0.6-V dynamic biasing filter with 89-db dynamic range in 0.18-µm CMOS. *IEEE J. Solid-State Circuits* **2009**, *44*, 2790–2799. [CrossRef]
18. Prommee, P.; Thongdit, P.; Angkeaw, K. Log-domain high-order low-pass and band-pass filters. *AEU-Int. J. Electron. Commun.* **2017**, *79*, 234–242. [CrossRef]
19. Sun, C.-Y.; Lee, S.-Y. A fifth-order Butterworth OTA-C LPF with multiple-output differential-input OTA for ECG applications. *IEEE Trans. Circuits Syst. II Express Briefs* **2018**, *65*, 421–425. [CrossRef]
20. Lee, S.-Y.; Wang, C.-P.; Chu, Y.-S. Low-voltage OTA–C filter with an area-and power-efficient OTA for biosignal sensor applications. *IEEE Trans. Biomed. Circuits Syst.* **2019**, *13*, 56–67. [CrossRef]
21. Grech, I.; Micallef, J.; Azzopardi, G.; Debono, C.J. A low voltage wide-input-range bulk-input CMOS OTA. *Analog Integr. Circuits Signal Process.* **2005**, *43*, 127–136. [CrossRef]
22. Pinto, P.M.; Ferreira, L.H.C.; Colletta, G.D.; Braga, R.A.S. A 0.25-V fifth-order Butterworth low-pass filter based on fully differential difference transconductance amplifier architecture. *Microelectron. J.* **2019**, *92*, 104606. [CrossRef]
23. Ghasemi, R.; Aminzadeh, H.; Ballo, A. Ladder-type G_m-C filters with improved linearity. *IEEE Access.* **2023**, *11*, 41503–41513. [CrossRef]